Tellus (2008), 60B, 188–199
Printed in Singapore. All rights reserved

TELLUS

Surface–atmosphere interactions over complex urban terrain in Helsinki, Finland

By TIMO VESALA[1]*, LEENA JÄRVI[1], SAMULI LAUNIAINEN[1], ANDREI SOGACHEV[1], ÜLLAR RANNIK[1], IVAN MAMMARELLA[1], ERKKI SIIVOLA[1], PETRI KERONEN[1], JANNE RINNE[1], ANU RIIKONEN[2] and EERO NIKINMAA[2], [1]*Department of Physical Sciences, P.O. Box 64, FIN-00014 University of Helsinki, Finland;* [2]*Department of Forest Ecology, P.O. Box 27, FIN-00014 University of Helsinki, Finland*

(Manuscript received 1 December 2006; in final form 1 July 2007)

ABSTRACT

Long-term measurements of fluxes of sensible heat (H), latent heat (LE) and carbon dioxide (F_c) were made from December 2005 to August 2006 over an urban landscape in Helsinki, Finland using the direct micrometeorological eddy covariance technique. Three distinguished sectors of land-use cover (vegetation, roads and buildings) allowed comparisons of fluxes over different urban surfaces. The normalized standard deviation of wind and scalars as a function of atmospheric stability were typical for rough surfaces, as were turbulence spectra and cospectra. Footprint analysis was performed by a boundary-layer one and half-order closure model allowing for discrimination of surface and canopy sinks/sources and complex topography. Fluxes were analysed as average diurnal courses over winter, spring and summer periods. H exceeded LE reaching 300 W m^{-2} over urban and road surfaces in the summer and it was close to 100 W m^{-2} in the winter. LE was highest in the summer over vegetation cover attaining 150 W m^{-2}. The emission rate of CO_2 was high over road sector [20 μmol (m^{2}s)$^{-1}$] [Correction added after online publication 16 Oct 2007: 30 μmol changed to 20 μmol] while in the vegetation sector it remained below 5 μmol (m^{2}s)$^{-1}$ and at summertime reached even -10 μmol(m^2 s)$^{-1}$ [Correction added after online publication 16 Oct 2007: wording of sentence altered]. Effluxes from soil measured by chambers were 1–3 μmol (m^{2}s)$^{-1}$. F_c correlated with traffic density and a background non-vehicle flux was 1 μmol (m^{2}s)$^{-1}$ [Correction added after online publication 16 Oct 2007: 2 μmol changed to 1 μmol].

1. Introduction

At the moment, the network of direct CO_2 flux measurements by the eddy covariance (EC) technique is rather dense for natural and semi-natural ecosystems (Baldocchi et al., 2001) while only a few measurements have been conducted over urban and suburban landscape. The longest urban record back to 2000 from the centre of Copenhagen is reported by Soegaard and Møller-Jensen (2003). Earliest measurements go back in the summer of 1995 (Grimmond et al., 2002), but the campaign undertaken in Chicago was only about 2 months long. Measurement periods in other studies vary in their length but no reported studies on European sites are from cities at high latitude (Nemitz et al., 2002; Grimmond et al., 2004; Salmond et al., 2005; Vogt et al., 2006) or they are from Japanese locations (Moriwaki and Kanda, 2004). No data from high latitudes ($>60^\circ$) is available. In one of the most recent papers, Vogt et al. (2006) came to the conclusion that the diversity of urban areas is not yet adequately covered by experimental studies and more long-term studies from variety of cities are needed. In December 2005 EC measurements of CO_2, sensible heat, latent heat and momentum fluxes started in Helsinki, Finland. Being at the latitude of 60°N it is presently the most northern urban flux tower site. The time series of this study covers the period from December 2005 to August 2006 and thus observations provide valuable information on temporal dynamics in the northern urban environment. Besides climatology, phenology is pronounced since the substantial fraction of the area close to the flux tower is covered by vegetation.

Emissions of CO_2 in the Helsinki area are estimated by Helsinki Metropolitan Area Council and in 2005 the main sources of CO_2 were energy plants with contribution of 72% (Myllynen et al., 2006). There are seven power plants and 27 heating plants in the Helsinki Metropolitan area and the yearly emissions were estimated to be 5101 t in 2005. The second largest source (17%) was traffic with yearly emission of 1241 t. In the whole Finland the estimated yearly CO_2 emissions from

*Corresponding author.
e-mail: timo.vesala@helsinki.fi
DOI: 10.1111/j.1600-0889.2007.00312.x

traffic have been modelled to be 11.97 MT in 2006 (Mäkelä et al., 2005). The city of Helsinki is very green; about one third of its surface area is parks and green areas. The urban vegetation in Helsinki is more variable in comparison to the natural vegetation at the hemiboreal Scandinavian vegetation zone where the city is located, with over 100 different tree species.

Urban environments are typically very heterogeneous and the roughness elements can be high. This often leads to the situation where classical micrometeorological preconditions of flux measurements (Roth, 2000) are compromised with practical limitations. For example the measurements may be carried out within the roughness sublayer close to canopy. Nevertheless, as pointed out by Vogt et al. (2006), the fluxes are real for the point in space where they are measured. Vogt et al. (2006) also unexpectedly observed that measurements at canopy top agreed with the Monin–Obukhov similarity theory better than those at tower top (2.2 times canopy height).

The presence of heterogeneities challenges the footprint analysis (e.g. Schmid, 2002). The source area size and upwind distance increase with thermal stability. Therefore, flux measurements can represent drastically different areas and mixture of surface classes at night and during daytime. Although simple analytical footprint models, such as the one by Schuepp et al. (1990) and Schmid (1994) have become widely used and integrated into EC software, their validity is restricted, strictly speaking, only to measurements carried out over an extended homogeneous surface with relatively short vegetation cover. The approach based on ensemble-averaged closure models of atmospheric boundary layer flow (Sogachev and Lloyd, 2004) allows for simulation of more realistic conditions of flow inhomogeneity, surface heterogeneities and topographical influences (Sogachev et al., 2004a), and of footprint estimates. One should pay special attention to this issue when interpreting results from complex sites. The measurements can be contaminated also by the effects of the local advection (e.g. Aubinet et al., 2005) although the EC method, since it is a method to measure turbulent, not advective fluxes, is somewhat robust against such effects (Eugster et al., 2003).

The main focus of this study is on the turbulent exchange of CO_2, sensible and latent heat fluxes over complex urban surface. Identification of the contrasts between three different land-use sectors (vegetation, roads and typical urban with high building cover) over three seasons (winter, spring and summer) is a crucial part of our study. This is aided by advanced modelling of footprint areas, where ground sources/sinks are treated separately from sources/sinks at elevated heights and effects of the local topography are included. Soil respiration is typically the most uncertain term in the land–ecosystem carbon balance and we determined the general level of soil respiration for vegetated surfaces by chamber measurements. The performance of EC method is demonstrated by spectral analysis and by the dependence of standard deviations on atmospheric stability.

Table 1. The land use fraction (λ) for three sectors within 250 m of the measurement tower

Wind sector	Type	λ_p	λ_r	λ_v
320–40°	Urban –with average building height (20 ± 2 m)	0.42	0.51	0.07
40–180°	Road	0.10	0.60	0.30
180–320°	Vegetation	0.02	0.13	0.85
All		0.14	0.40	0.46

2. Materials and methods

2.1. Site and measuring platform

A 31 m high triangular lattice tower was established in autumn 2004 (60°20′ N, 24°96′ E) as a part of urban measuring station Station for Measuring Ecosystem – Atmosphere Relationships (SMEAR III). The tower is located on a hill (26 m above sea level) (see Fig. 5) about three kilometers northeast from downtown of Helsinki. The surrounding area is very heterogeneous consisting of buildings, patchy forest and low vegetation, parking lots and roads. The surface can be classified to three sectors: urban (mostly buildings and roads including parking lot), road (mainly roads) and vegetation (mainly low vegetation) (Table 1). Within the radius of 250 meters around the measuring tower the fraction covered by vegetation (λ_v) is 0.46, roads (λ_r) 0.4 and buildings (λ_p) 0.14. Most of the buildings are located in the urban sector where a high plane area density (plane area of roughness elements relative to total surface area) is 0.42. The average height of the buildings is 20 m and they resemble commercial buildings. The closest building is located in the road sector about 28 m away in the direction 60–110° but its average height is only 7 m. The distance between the tower and the closest of the high buildings is 55 m. The greenspace in the southwest consists mainly of grasses and garden cultivation in an allotment garden and in University Botanical Garden. The belt of deciduous trees, mainly birch (*Betula* sp.), Norway maple (*Acer platanoides*), aspen (*Populus tremula*), goat willow (*Salix caprea*) and bird cherry (*Prunus padus*), is 50–150 m away from the tower. Indigeous soils in the area are predominantly rock and till in the hill area and till or clay in low-lying areas. The displacement height d can be estimated from the relationship two-third times the main canopy height (Grimmond and Oke, 1999). For urban sector d was 13 m and for road and vegetation sectors 8 and 6 m, respectively.

The prevailing wind direction was southwest and the average of half-hourly averages wind speed was 3.1 m s^{-1} over the studied period from December to August. The corresponding average temperature was 5.5 °C with the minimum and maximum temperatures of −23.2 and 28.2°C. The average relative humidity was 71% and the average global radiation was 143 W m^{-2}. The measuring period was meteorologically typical excluding

the very low precipitation in the summer. The summer was also warmer than on average.

2.2. Meteorological and eddy covariance measurements

Weather conditions were monitored by a Milos 520 weather station (Vaisala Ltd.) at the roof of the building Physicum 26 m above ground, about 220 m northeast from the tower. The eddy covariance (EC) set-up included a Metek ultrasonic anemometer (USA-1, Metek GmbH, Germany) to measure the three wind speed components and sonic temperature, and an open-path infrared gas analyser (LI-7500, Li-Cor Inc., Lincoln, Nebraska, USA), which measures CO_2 and H_2O concentrations. The measurement height was 31 m and sampling frequency was 10 Hz. The gas analyser was connected to the anemometer data logger for synchronization. The raw data were stored for later post-processing. The turbulent fluxes of sensible heat, CO_2, H_2O and momentum were calculated as covariances between the scalars (temperature or mixing ratio) or horizontal wind speed and vertical wind speed according to commonly accepted procedures (Aubinet et al., 2000). The 3-D rotation was adopted for calculation of final flux values. 3-D rotated values were compared with 2-D rotated values and those calculated by the planar-fitting method (Wilczak et al., 2001). In planar-fitting, streamline coordinates are determined based on the measured statistics of the wind field. The flux correction caused by water vapour and sensible heat transfer was performed according to Webb et al. (1980). We also tested the effect of the correction resulting from the surface heating of the open-path gas analyser (Burba et al., 2006). Since the main focus of this study is on average behaviour and especially daytime fluxes, no storage fluxes were calculated. Spectra were calculated using fast Fourier transform (FFT) on segments of 2^{14} data points (about 27 min), which were linearly detrended and Hamming windowed (Kaimal and Kristensen, 1991). The fluxes were averaged over 30-min periods (unless otherwise mentioned) with linear detrending of time series. The monthly mean diurnal patterns were further constructed from half hour basic data. Turbulent spectra are based on 150-min data.

2.3. Soil respiration measurements

The soil CO_2 fluxes were measured during a 2 d campaign in 18 and 19 September 2006 with a portable closed chamber CO_2 measurement system described by Kolari et al. (2005), which uses a Vaisala CO_2—analyser (GMP343, Vaisala Ltd., Vantaa, Finland). The chamber was covered with aluminium foil to prevent light from penetrating into the chamber. Measurements were made in eight different locations which were representative for the surrounding vegetation. Two locations were on the forested hill and others were in greenspace around the tower. These included measurements from grass and cultivated garden (e.g. onion, pea and strawberry). One measurement lasted 5 min and CO_2 concentration was measured every 5 s. We made two measurements at every location at two different times of day. The CO_2 flux from the soil was calculated from the average concentration increase corrected for air pressure and temperature effects. Note that chambers provide spot measurements on a limited number of soil types and results should be thus treated with caution.

2.4. Footprint analysis

Footprint analysis was performed using the numerical atmospheric boundary-layer model SCADIS (Sogachev et al. 2004a; Sogachev and Lloyd, 2004; Sogachev and Panferov, 2006). The model is based on a one-and-a-half-order turbulence closure applying a $E-\omega$ scheme (where E is the turbulent kinetic energy and ω is the specific dissipation of E) (Sogachev et al., 2002, 2004b). Building areas were parameterized as canopy layers with appropriate heights and densities similarly to Sogachev and Panferov (2006). Forcing of the flow in the model was provided using a prescribed geostrophic wind of 10 ms^{-1} at the upper boundary of the model domain at the height of 2 km. Here, we assumed a neutral stratification in all model runs, since model simulations in stable cases are more uncertain and the assumption of the neutral stratification provides conservative estimates for unstable cases, that is neutral footprints are larger than unstable ones. The model ignores the anthropogenic heat output. The footprints were estimated for two wind directions of 110° and 250°, which represent road and vegetation sectors, respectively (Table 1), and separately for sinks/sources located on the ground (soil and traffic) and in the canopy (effective sources located approximately at the height of d).

2.5. Analysed periods and data selection

The analysed period started on 1, December 2005 and ended on 31, August 2006. The record was divided into three seasons: winter (December to March,) spring (April–mid-May) and summer (mid-May–August). The analyses were made separately for three different sectors (Table 1). The results concerning micrometeorological characterization of the surface and turbulence parameters over the urban sector must be taken with caution since the buildings are located close to the tower and their mean height is two thirds of the height of the tower. However, the flux estimates were more robust.

A significant source of bias in long-term EC-based carbon balance estimates is the apparent dependence of the flux on the friction velocity. For forest sites, EC fluxes even after storage correction have been observed to decrease at low friction velocities, typically during calm nights (Aubinet et al., 2000). This behaviour was not observed in this study and data was not filtered against the friction velocity. All measurements points with the friction velocity of less than 0.1 m s^{-1}, only few of them, were omitted. Clear peaks were removed by visual inspection

and after this a stationarity test was performed according to the method by Foken and Wichura (1996), where the 30-min interval used for a calculation of a single flux value was divided into shorter intervals (5-min subrecords). If there was a difference of less than 30% between the mean covariances of subrecords and the covariance of the full period, the measurement was considered stationary, otherwise it was rejected as non-stationary. The minimum amount of rejected data was 32% for winter momentum and sensible heat fluxes and the maximum amount was 65% for winter carbon dioxide fluxes. Breaks in measurements contributed to 10–15%. Most omissions were due to unsatisfied quality criteria. The fraction of the rejected data was high, but it is normal that 20–30% and 50–60% of eddy covariance day- and night-time data, respectively, is rejected (e.g. Suni et al., 2003) and further gap-filled. No gap-filling was attempted here due to the complex nature of the CO_2 exchange above urban surfaces.

3. Results and discussion

3.1. Surface and turbulence characteristics

We first consider effects of rotation angles and planar fitting on flux estimates. Planar fitting was based on 20 wind direction bins that is 18 classes of streamline coordinates. The vertical rotation angle (azimuth angle) as a function of the wind direction is presented in Fig. 1. The angle indicates the slope of surrounding surface (positive value meaning downward from the tower) and it did not exceed 12°. The values were in agreement with the local topography excluding the northern sector, where massive institute buildings are located. These probably modify flow field and create artefacts in the rotation angle. In addition, the anemometer is in the wake of the measurement tower in the directions of 0–60°. The complex terrain may also lead to dissimilarities between different rotation options used in the flux calculation. Figure 2 shows the fluxes averaged over June–July as a function of the wind direction calculated by 2-D and 3-D rotations and planar-fitting method. The planar-fitted fluxes were generally somewhat smaller (in the case of the momentum flux closer to zero) than those obtained by the ordinary rotations. For the momentum flux the difference appeared with the same magnitude in all directions whereas in the energy fluxes the largest

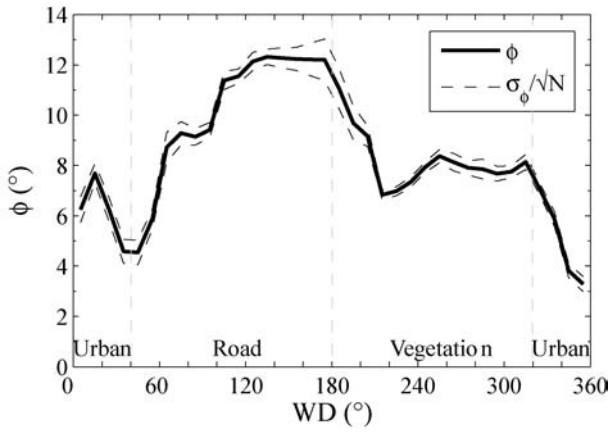

Fig. 1. Rotation angle as a function of the wind direction (10° averages). The dashed line shows the standard error.

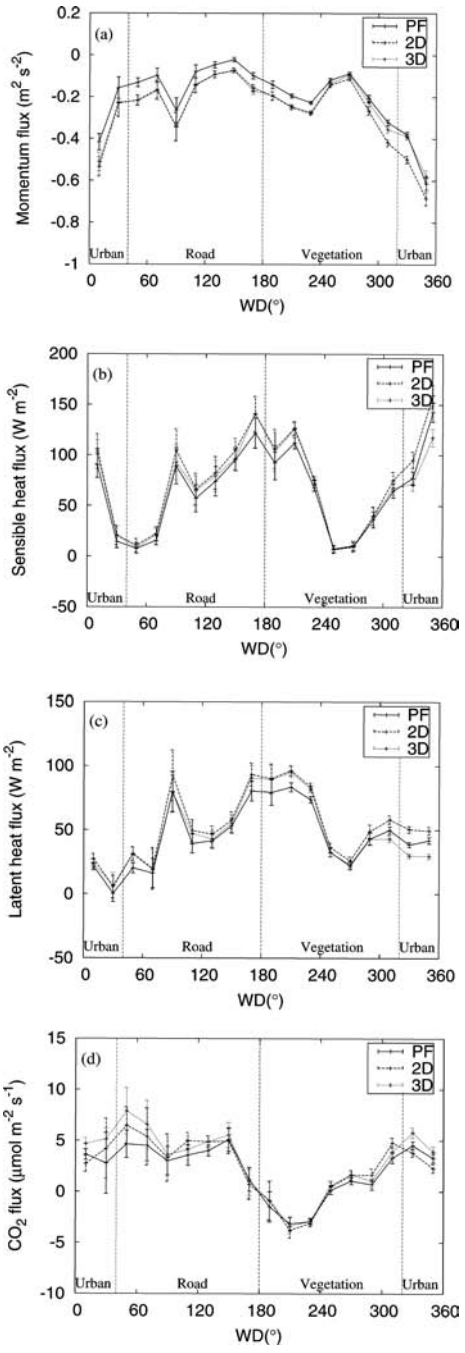

Fig. 2. Fluxes calculated by 2-D and 3-D rotations and by planar fitting (solid line) for June–July period. Note that in many cases 2-D and 3-D rotations are difficult to distinguish since they are very close to each other.

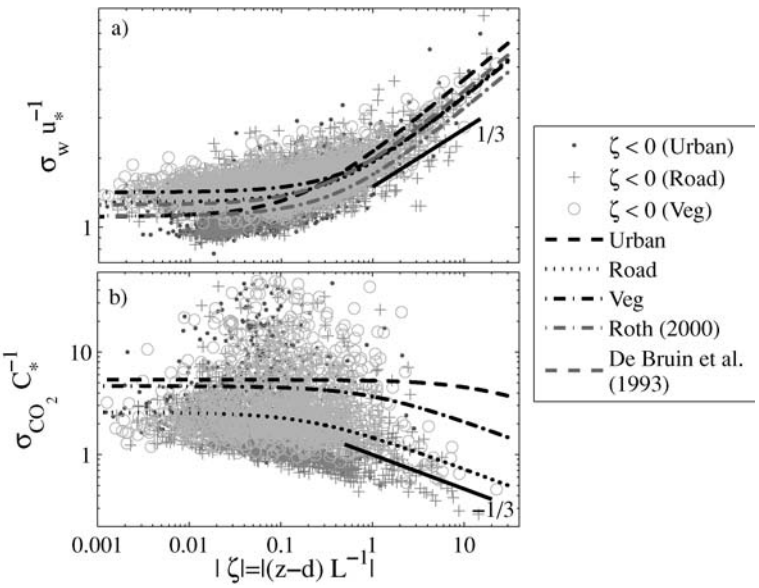

Fig. 3. The normalized standard deviation of a) vertical velocity w and b) CO_2 concentration as a function of stability for the three wind sectors. For urban sector (dashed) the least-square fits gave $\sigma_w/u_* = 1.1 \cdot (1 - 6.2\zeta)^{1/3}$ and $\sigma_{CO_2}/C_* = 5.4 \cdot (1 - 0.1\zeta)^{-1/3}$. For road sector (dotted) these were $\sigma_w/u_* = 1.3 \cdot (1 - 2.4\zeta)^{1/3}$ and $2.6 \cdot (1 - 4.5\zeta)^{-1/3}$. Fittings $\sigma_w/u_* = 1.4 \cdot (1 - 1.7\zeta)^{1/3}$ and $\sigma_{CO_2}/C_* = 4.7 \cdot (1 - 0.1\zeta)^{-1/3}$ were received for vegetation sector (dash–dotted) [Correction added after online publication 16 Oct 2007: values in this section have been altered]. See Table 2 for more accurate values of fitted parameters.

differences occurred in the direction of the sloped terrain and the most abrupt roughness change (around 200°) and of buildings (over 300°). For CO_2 flux, the effect of the buildings was dominant. The analysis revealed that the vertical velocity fluctuations by planar-fitting were smaller than by standard methods leading to systematically lower turbulent flux estimates. Over a very complex terrain, the different rotation methods seemed to lead to differences in fluxes of the order of 10%. However, the general analysis concerning the dynamics of the fluxes and main conclusions presented later are not sensitive to the differences shown in Fig. 2. The results presented below are based on the 3-D rotation.

The normalized standard deviations of wind velocity components and scalars were analysed as a function of atmospheric stability for all three land use sectors. According to Monin–Obukhov Similarity (MOS) theory (e.g. Foken, 2006), when the variances of atmospheric scalars and parameters are normalized with the corresponding flux parameters, they became functions of dimension length ζ. Only unstable conditions ($\zeta < 0$) were analysed and plotted. In addition, equation $\frac{\sigma_x}{x_*} = C_1(1 - C_2\zeta)^{C_3}$, where $\zeta = (z–d)/L$, C_1, C_2 and C_3 are empirical constants and L is the Obukhov length derived from the EC measurements, was fitted to the data. In the case of wind velocity components, the divisor is friction velocity u_* and for scalar s it is $s_* = \frac{-\overline{w's'}}{u^*}$, where s' and w' are the instantaneous deviations from the time-averaged values of the mixing ratio and vertical wind component, respectively, and the bar above the product of the fluctuations denotes time averaging.

The normalized standard deviations for vertical velocity w are shown in Fig. 3a and the values of the constants from the fittings are listed in Table 2. Reference fittings over urban (Roth, 2000) and rural sites (De Bruin et al., 1993) are also shown in Fig. 3. The estimated values of C_1 factors for w broadly agreed with typical values over complex terrain, showing a decrease with increasing plane area of buildings. This is due to the higher momentum transfer resulting from higher roughness (Roth and Oke, 1995). We made the sensitivity tests for the factor C_3 by keeping the factor in fixed value of 1/3 or letting it be one of the factors to be fitted. Within the unstable regime the data followed the 1/3 power law for all sectors, although the scatter was notable. The stability dependence was most distinct in urban sector and lowest in vegetation sector. The normalized standard deviations of horizontal wind components did not follow the 1/3 power law but were otherwise in accordance with MOS-theory and deviations between different sectors were smaller (not shown).

Table 2. The fitting coefficients for normalized standard deviation regressions of vertical wind velocity and carbon dioxide concentration, for three different sectors

Land use		C1	C2	C3
Urban	w	1.11	6.18	1/3
	CO_2	5.36	0.06	−1/3
Road	w	1.28	2.39	1/3
	CO_2	2.58	4.49	−1/3
Vegetation	w	1.42	1.68	1/3
	CO_2	4.65	1.01	−1/3

[Correction added after online publication 16 Oct 2007: values in Table 2 have been changed].

The normalized standard deviations of carbon dioxide against ζ are shown in Fig. 3b and constants from fittings are listed in Table 2. For the road sector a near-neutral value of the factor C_1 for CO_2 was estimated to be 2.6, while the urban and vegetation sectors showed similar values 5.4 and 4.7, respectively. In the unstable regime the data for all sectors followed the expected

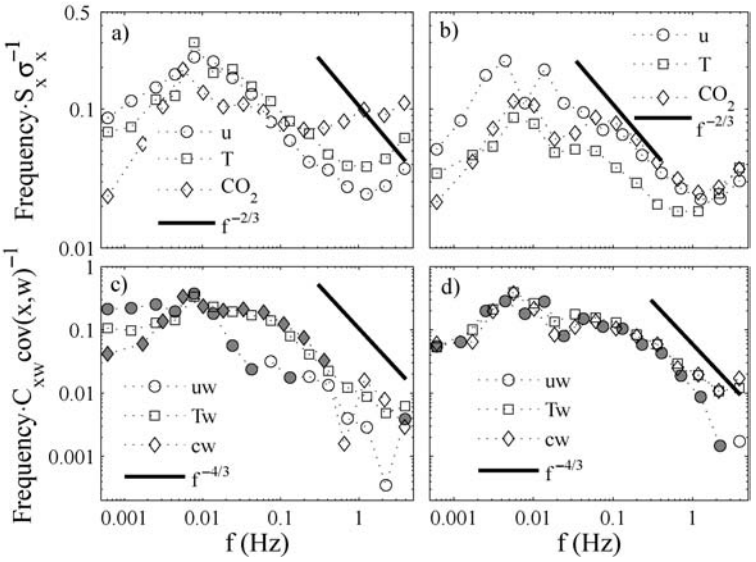

Fig. 4. Turbulence spectra of u, T and CO_2 and cospectra of uw, Tw and $c_{CO_2}w$ in two different land use sectors (vegetation and urban). In (a) and (c) are spectra and cospectra, respectively, from 1200 to 1430 on 30, May 2006 with mean wind speed 4.0 m s^{-1}, wind direction southwest (vegetation) and Obukhov length −27 m and in (b) and (d) are spectra and cospectra, respectively, from 1300 to 1530 on 9, May 2006 with mean wind speed 2.7 m s^{-1}, wind direction North (urban) and Obukhov length −267 m. In covariances the filled markers indicate downward fluxes. Also the power law $f^{-2/3}$ and $f^{-4/3}$predicted by Kolmogorov for power spectra and cospectra were plotted.

−1/3 power law. Other studied scalars, temperature and water vapour concentration, decreased according to the −1/3 power law in all sectors (not shown). [Correction added after online publication 16 Oct 2007: the above paragraph has been altered].

We calculated the power spectra and cospectra for two land use sectors. The time period representing flow from the vegetation sector was between 1200 and 1430 on 30, May 2006. The average wind speed was 4.0 m s^{-1}, wind direction was from southwest and Obukhov length was −27 m. During the time period from 1300 to 1530 on 9, May 2006 flow was from urban sector. Average wind speed was 2.7 m s^{-1}, wind flow was most of the time from North turning to southeast and Obukhov length was −267 m. Power spectra and cospectra were normalized with variances and covariances, respectively, and plotted as a function of frequency in logarithmic axes. The power spectra of rotated u-component, temperature T and CO_2 were studied (Fig. 4a and b) with cospectra of momentum, heat and CO_2 flux (Fig. 4c and d).

In the vegetation sector the power spectra of u and T had very similar behaviour (Fig. 4a). Both peaked around 0.008 Hz and the inertial subrange followed the −2/3 power law between 0.02 and 1 Hz. The power spectrum of CO_2 peaked at somewhat lower frequency (0.0055 Hz) and did not follow the power law. The broader shape of the CO_2 variance spectrum due to noise at high frequencies may have contributed to the level of the CO_2 variance in Fig. 3b. The energy was more evenly distributed to different sized eddies in the case of CO_2 than u and T. In the urban sector the power spectrum of u-component showed a bimodal pattern, first at frequency of 0.0045 Hz and second at 0.015 Hz (Fig. 4b). The spectra of T and CO_2 peaked at the same frequency range of 0.005–0.007 Hz. The probable effect of the spectral shortcut due to the building wake effect could be seen as a step between 0.04 and 0.1 Hz especially in the case of T and CO_2. According to Taylor's hypothesis (e.g. Stull, 1988), which assumes that mean wind speed divided by the frequency gives an estimate for a size of the eddy the frequency represents, these frequencies correspond to eddy sizes of 68 m and 27 m, respectively, which are of same order as building sizes. All power spectra followed the −2/3 power law between 0.1 and 1 Hz (excluding CO_2 signal in Fig 4a, where more noise appears at high frequencies).

All cospectra peaked at frequency range 0.005–0.009 Hz in the direction of high vegetation cover (Fig. 4c). The Tw and c_{CO_2} w spectra followed the −4/3 power spectra in the inertial subrange. The uw spectrum was first decreasing faster and then slower than the power law. More energy was in larger eddies in the case of momentum flux than in the case of heat flux and CO_2 flux. The cospectra of different fluxes behaved similarly in the direction of buildings (Fig. 4d). They all peaked at same frequency range as in vegetation sector. All cospectra followed the Kolmogorov's power law at the higher end of the inertial subrange (0.1–1 Hz). A step due to the wake effect was detected in all covariances at frequency range 0.02–0.08 Hz. The comparison of CO_2 cospectra in different flow situations revealed a different behaviour. All eddies regardless of the size indicated upward transport in the urban sector where no large carbon sinks exist. In the vegetation sector larger eddies transported downward flux component and smaller upward. The dominantly downward flux components exist in this direction since vegetation is a sink at daytime.

As a summary, the power spectra and cospectra followed common spectral behaviour reasonably well in both situations. We did not detect the peak shifting due to wake effect in the urban sector often observed in urban areas (Roth, 2000). However, when comparing the behaviour in low frequency end between different sectors, a steeper decrease was observed in power spectra of u and T and in cospectra of uw and Tw for a flow over the urban sector.

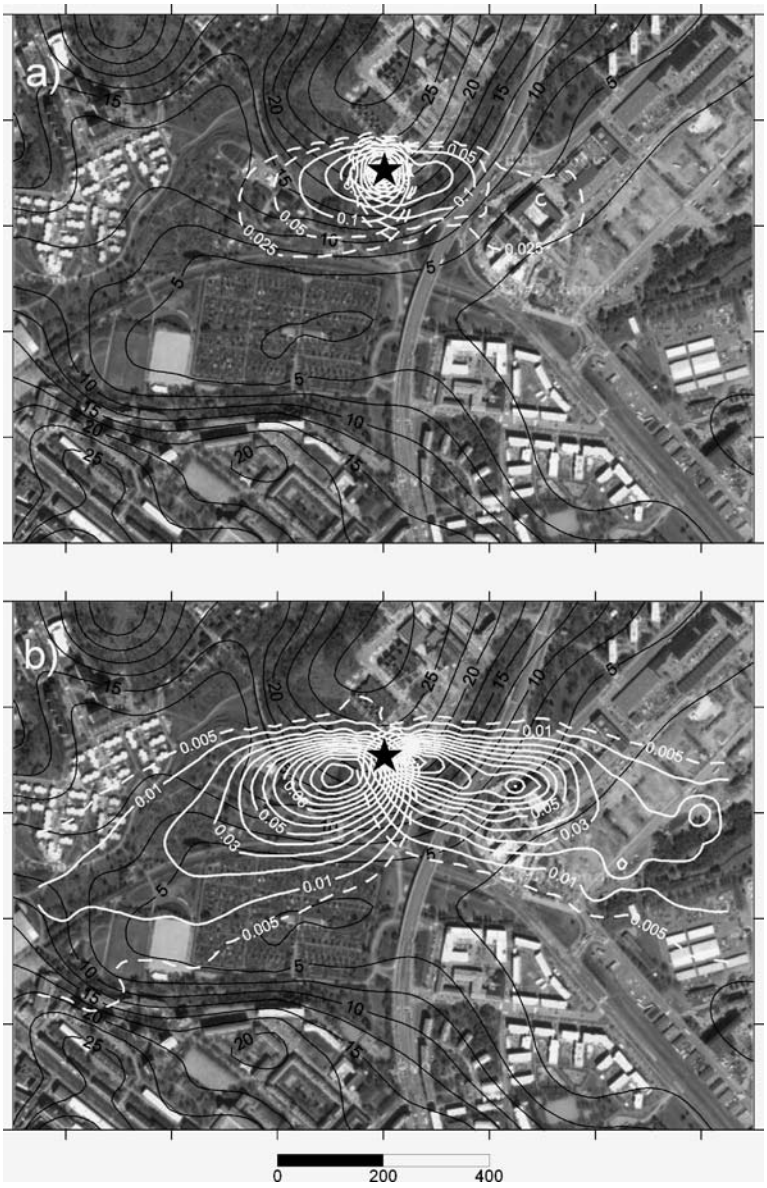

Fig. 5. Topography of the measurement site is drawn by black contours. White contours give footprints for (a) canopy (upper) and (b) soil (lower) sources: scale (10^{-4} m^{-2})

3.2. Footprints

By footprint analysis we can estimate the contribution of different surface cover into a signal registered at the tower. Fig. 5 illustrates the source area distributions in the directions of road and vegetation sectors and for canopy and ground sources/sinks. The heterogeneity of urban surface results in complex transport from sources to receptor and the footprint signature was asymmetric along prevailing wind direction. Thus any two-dimensional footprint models (especially based on analytical solutions) should be avoided for urban surrounding even with flat topography. There exists also a difference between footprints for ground sources and elevated ones, which is addressed for forest simulations by, for example, Markkanen et al. (2003) and Finnigan (2004). The canopy footprints were much smaller in size than ground ones. Based on the footprint estimates, the contribution of building, road and vegetation area in the Easterly sector (road) to canopy exchange was 10, 21 and 69%, respectively, and to ground exchange 12, 32 and 20%. Mathematically, the surface area of influence on the entire flux goes to infinity and thus one must always define the percentage level for the source area. Here the simulated source area contributing to the flux measurement was 64%. The contribution of building, road and vegetation area in the vegetation sector (southwest) to canopy exchange was 5, 1 and 94%, respectively, and to ground exchange 9, 1 and 58%. Here the simulated source area contributing to the flux measurement was 69%. Note that these source area fractions give solely the contributions of each cell of surface without any weighting with the source/sink strength. Although the fraction of road cover in the road sector was only 20–30%, the contribution of the traffic

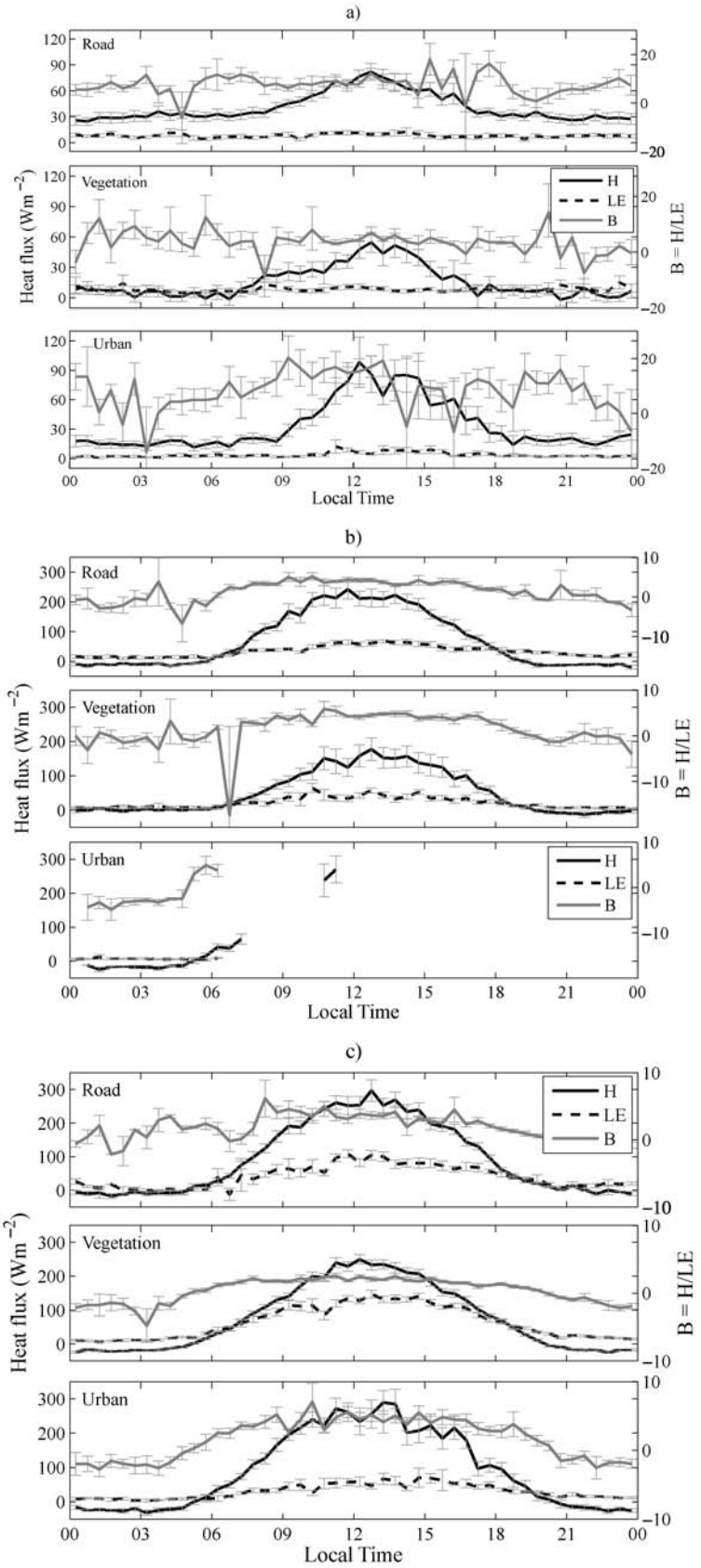

Fig. 6. Sensible H and latent heat LE fluxes and Bowen ration B (right axis) for winter (a), spring (b) and summer (c) in the three different sectors. Bars represent the standard errors. Data coverage of spring-time urban sector is low since the spring period was rather short and wind is seldom from that direction.

to the measured CO_2 signal is higher since traffic source strength of CO_2 is very large, about 60 000 vehicles per day (Lilleberg and Hellman, 2006).

3.3. *Heat fluxes and Bowen ratio*

Fig. 6. presents the diurnal sensible (*H*) and latent (*LE*) heat fluxes and *H/LE* (the Bowen ratio) averaged over three seasons and the three sectors. The *H* always exceeds *LE* reaching 300 W m^{-2} during summer daytime over urban and road sectors. In winter, the daytime maximum was close to 100 W m^{-2}. *H* flux over vegetation was systematically somewhat lower, since in the summer the heat consumed in transpiration decreases the flux and in the winter the anthropogenic sources increased *H* over roads and buildings. The negative sign of *H* indicates stable stratification which appeared most of the time during spring and summer nights, when the fluxes were about −30 to −20 W m^{-2}. During winter nights the urban and road sectors remained slightly unstable while the stratification over the vegetation patch was more neutral. Nocturnal urban boundary layers may often be unstable (Salmond et al., 2005). Our results can be compared to those reported in earlier urban studies. In Basel in summer over a street canyon, *H* was almost always directed upward with peak values around 400 W m^{-2} (Vogt et al., 2006). Grimmond et al. (2004) presented summer data from Marseille, where the mean daily *H* was around 150 W m^{-2} and around 250 W m^{-2} during the period when the net radiation was positive. In residential area of Tokyo, the peak value of *H* was about 300 W m^{-2} at midday in July (Moriwaki and Kanda, 2004).

LE (Fig. 6) exhibited a pronounced diurnal cycle in the summer. *LE* tended to increase towards the spring and further to the summer over all surfaces. During the summer *LE* reached 150 W m^{-2} at the vegetation sector due to increased transpiration. For a pine-forest in the similar climatic conditions (200 km to the North from Kumpula site) the reported values are below 200 W m^{-2} (Markkanen et al., 2001; Suni et al., 2003) being close to those obtained for the urban site. Rannik et al. (2002) studied a forest clearing nearby the pine forest site and the maximum value of the average diurnal *LE* was about 50 and 30 W m^{-2} for July–August and September, respectively. Grimmond et al. (2002) presented *LE* data from 10 urban sites and found that daily maximum varied from about 20 to 250 W m^{-2}. Summertime Basel-measurements by Vogt et al. (2006) revealed that *LE* was generally below 100 W m^{-2}. In Marseille in the summer the mean *LE* was about 50 W m^{-2} (Grimmond et al., 2004). In Tokyo the mean hourly *LE* for sunny summer days reached 200 W m^{-2} (Moriwaki and Kanda, 2004) and daily average wintertime flux was around 14 W m^{-2}.

Fig. 6 presents also the ratio of the energy fluxes, that is, the Bowen ratio. The wintertime values were overall largest since the evapotranspiration is small. The ratio reduced below 5 during spring period. In winter the Bowen ratio over the vegetated surface was generally smallest, whereas in the spring the road and vegetation sectors were more similar. In summer time the effect of vegetation in reducing Bowen ratio was evident. Markkanen et al. (2001) reported for pine-forest Bowen ratio values (200 km to North) up to 7 in cold, winter April and daytime values of around 1 for July. Considering that conifers tend to transpire less than broad-leaf trees, the values obtained now for the urban surface are consistent with the pine forest observations. Grimmond et al. (2002, 2004) presented midday Bowen ratios as a function of vegetation cover for 10 North American urban sites and Marseille. The ratio varied from about 1 to 30 reflecting probably differences in land cover and water availability. Nemitz et al. (2002) showed that the late-autumn *H* and *LE* at Edinburgh were maximally 100 W m^{-2} while Bowen ratio was about 1. In the summer daytime in Tokyo, the ratio was about 1.8 exceeding 3 in winter (Moriwaki and Kanda, 2004).

3.4. *Carbon dioxide fluxes*

Figure 7 shows the net carbon dioxide exchange for three seasons over three surface types. The surroundings of the flux tower acted as an overall source of carbon (excludind vegetation sector in summer) and a clear dependence on the surface cover was distinguishable. The road sector exhibited the largest emissions rates with a marked diurnal cycle. This pattern remained the same from season to season. In summer, all sectors manifested diurnal cycle with lowered fluxes in daytime. The average carbon dioxide fluxes together with 5 and 95% percentiles are shown in Table 3. The table lists also values which were corrected according to Burba et al. (2006) for sensor heating effects. The correction was most significant in the winter. The average road emissions are rather stable from season to season. The lowest seasonal-averaged value was −1.2– −0.6 μmol (m^{2}s)$^{-1}$ for the spring over the vegetation sector and the highest was 11–12 μmol (m^{2}s)$^{-1}$ for the spring from the road sector. The most negative −5% percentile during the whole period was −5 μmol (m^{2}s)$^{-1}$ and the highest 95% percentile was 31 μmol (m^{2}s)$^{-1}$ in the spring from the traffic. [Correction added after online publication 16 Oct 2007: the above paragraph has been altered].

Moriwaki and Kanda (2004) have collected emission data based on EC measurements from densely built-up Basel (Vogt et al., 2003), suburban Chicago (Grimmond et al., 2002) and city centre Edinburgh (Nemitz et al., 2002) besides their own measurements over residential Tokyo. Highest emission rates up to 75 μmol (m^{2}s)$^{-1}$ were found at Edinburgh while the lowest maximum values of around 10 μmol (m^{2}s)$^{-1}$ were detected at Tokyo in summer and Chicago. The lowest flux in Tokyo was about 5 μmol (m^{2}s)$^{-1}$ and in other sites 0 μmol (m^{2}s)$^{-1}$. Basel measurements were reported also by Vogt et al. (2006) and the fluxes on average always directed upward being lowest of about 3 μmol (m^{2}s)$^{-1}$ in the night and reaching 14 μmol (m^{2}s)$^{-1}$ during daytime. Grimmond et al. (2004) reported measurements above the centre of Marseille in summer. The city district was found to be almost always a source [up to around 40 μmol (m^{2}s)$^{-1}$]

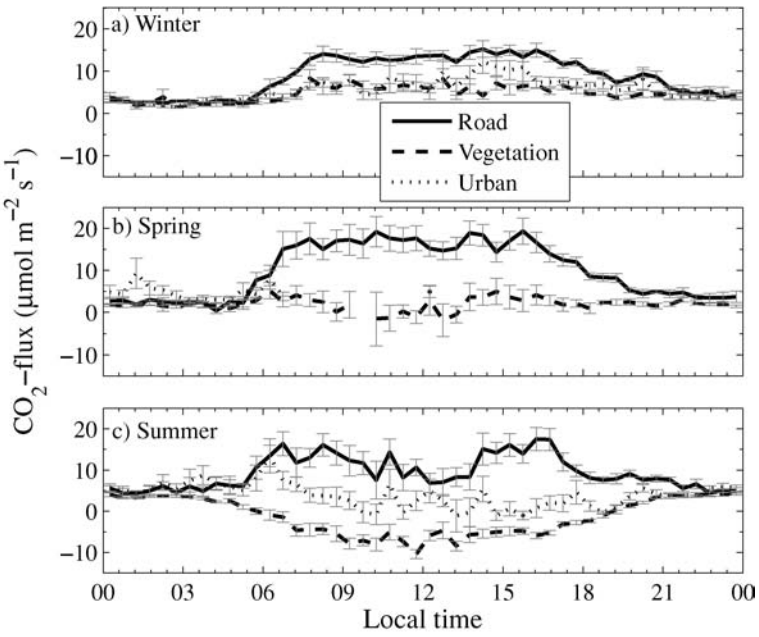

Fig. 7. Carbon dioxide exchange for three seasons over the three different sectors. Bars represent the standard errors.

Table 3. Average fluxes over three seasons and 5 and 95% confidence intervals. The values on parenthesis are estimated after the correction by Burba et al. (2006) [Correction added after online publication 16 Oct 2007: the values in the belew table have been changed].

		Average CO_2 flux [μmol $(m^2s)^{-1}$]	5% percentile of of CO_2 flux [μmol $(m^2s)^{-1}$]	95% percentile of CO_2 flux [μmol $(m^2s)^{-1}$]
Winter	Urban	5.45 (8.14)	0.01 (2.68)	14.11 (16.67)
	Road	9.34 (11.81)	1.85 (3.66)	21.27 (24.43)
	Vegetation	4.72 (6.63)	0.56 (2.37)	13.93 (15.82)
Spring	Urban	4.14 (4.83)	0.50 (1.01)	9.80 (10.48)
	Road	10.96 (12.02)	0.97 (2.00)	30.61 (31.45)
	Vegetation	2.00 (3.24)	−3.53 (−2.72)	8.36 (10.17)
Summer	Urban	4.76 (5.37)	−3.36 (−3.13)	17.92 (18.52)
	Road	10.36 (10.65)	−0.81 (−0.29)	27.00 (27.08)
	Vegetation	−1.22 (−0.62)	−13.14 (−12.53)	6.57 (7.32)

but the vegetation reduced the fluxes in the afternoon similarly to Helsinki. Finally, in Copenhagen, Søgaard and Møller-Jensen (2003) reported the emission rates from less than 5 μmol $(m^2s)^{-1}$ in the residential areas up to 100 μmol $(m^2s)^{-1}$ along the major roads in the city centre.

The soil chamber measurements indicated that the respiration level of the treeless vegetation surface was from 1 to 3 μmol $(m^2s)^{-1}$. The largest values were measured at a kitchen garden and lowest at herbaceous border. The chamber measurements were close to nocturnal vegetation sector EC estimates. Note that the night-time emissions were on approximately the same level regardless of the season. According to Markkanen et al. (2001) the net ecosystem exchange of the pine forest (200 km to North) varies from summer-day minimum of about –20 μmol $(m^2s)^{-1}$ to summer-night maximum of about 10 μmol $(m^2s)^{-1}$. [Correction added after online publication 16 Oct 2007: the previous paragraph has been altered].

Finally, we correlated the hourly carbon dioxide fluxes since 1, January 2006 with traffic density obtained from traffic counts (Fig. 8). Only flow situations from the road sector 40–180° were analysed. The traffic density was obtained for one of the main roads (Itäväylä) and the traffic density was correlated with the main road in the flux tower area (Hannu Seppälä, Helsinki City Planning Department, personal communication, 2006). The intercept of the regression, which indicates non-vehicle sources, is 1.1 μmol $(m^2s)^{-1}$ [Correction added after online publication

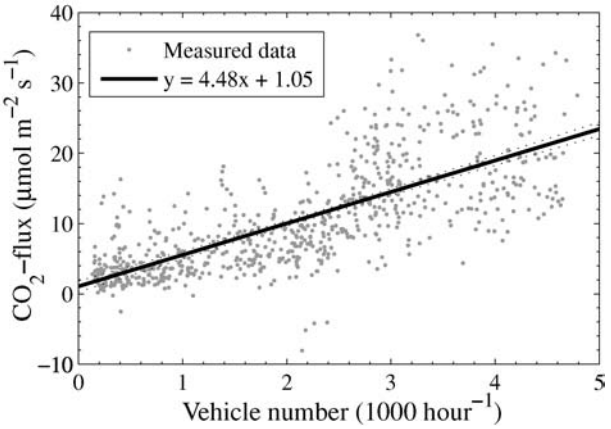

Fig. 8. Carbon dioxide exchange vs. the traffic density. The line is the linear fitting to the data points [function $y = y(x)$] and the dashed lines show 95% confidence bands for the measured flux.

16 Oct 2007: the value was previously 2.0 μmol $(m^2s)^{-1}$], while Nemitz et al. (2002) reported 12 μmol $(m^2s)^{-1}$ from a similar analysis in Edinburgh city centre. This is a consistent result since non-vehicle sources can be expected to be larger in the centre of Edinburgh than at the site of this study. For example, the district heating is very common in Helsinki reducing the local anthropogenic CO_2 sources, compared with Edinburgh, where most residential and institutional buildings include their own heating appliances. The intercepts of the regressions for winter and summer data separately are 2.5 and 1.6 μmol/(m^2s) (not shown). [Correction added after online publication 16 Oct 2007: these values have been changed from 4.1 and 3.0, respectively].

4. Conclusions

The site of our study was characterized by complex urban terrain with heterogeneities in surface cover and non-flat topography. However, the basic features of the Monin–Obukhov Similarity theory for the dependence of standard deviation of wind and scalars on atmospheric stratification were roughly valid with similar parameters to previous studies conducted in urban landscape (De Bruin et al., 1993; Roth, 2000). Turbulent spectra and cospectra followed Kolmogorov's theory and showed similar behaviour as observed also in other urban and forest environments (e.g. Constantin et al., 1999; Roth, 2000). The complex environment requires a sophisticated tool for source area analysis in contrast to measurements over flat low-vegetation surface, for which even the analytical footprint models are applicable. The boundary-layer closure model applied in this study allowed 3-D mapping of the concentration and flow fields, from which the footprint functions for vertically distributed sources/sinks can be deduced. The records of sensible heat, latent heat and carbon dioxide fluxes by the EC were northernmost reported. We observed clear seasonal and diurnal effect cycles with the pronounced of the vegetation lowering CO_2 fluxes in summer. Chamber measurements revealed soil respiration rates in agreement with EC observations. Our results regarding general level of emissions and variations in Helsinki resemble those reported earlier at lower latitudes. The maximum emissions in Helsinki remained smaller than those detected in Copenhagen, Edinburgh and Marseille but were larger than those in Basel, Chicago and Tokyo. [Correction added after online publication 16 Oct 2007: the previous paragraph has been altered].

5. Acknowledgments

The study was supported by EU project Carboeurope, Nordic Centre of Excellence NECC, REBECCA by Helsinki University Environmental Research Centre (HERC) and Research Foundation of the University of Helsinki. Liisa Kulmala is thanked for providing help in chamber measurements.

References

Aubinet, M., Berbigier, P., Bernhofer, Ch. Cescatti, A., Feigenwinter, C. and co-authors. 2005. Comparing CO_2 storage and advection conditions at night at different carboeuroflux sites. *Boundary-Layer Meteorol.* **116**, 63–93.

Aubinet, M., Grelle, A., Ibrom, A., Rannik, Ü., Moncrieff, J. and co-authors. 2000. Estimates of the annual net carbon and water exchange of European forests: the EUROFLUX methodology. *Adv. Ecol. Res.* **30**, 114–175.

Baldocchi, D., Falqe, E., Gu, L. H. Olson, R., Hollinger, D. and co-authors. 2001. FLUXNET: A new tol to study the temporal and spatial variability of ecosystem-scale carbon dioxide, water vapour, and energy flux densities. *Bull. Amer. Meteorol. Soc.* **82**, 2415–2434.

Burba, G., Anderson, D., Liukang, Xu and McDermitt, D. 2006. Correcting apparent off-season CO2 uptake due to surface heating of an open path gas analyzer: progress report of an ongoing study. *Proceedings of 27th Annual Conference of Agricultural and Forest Meteorology*, Amer. Met. Soc., San Diego, California, USA, pp. 1–13.

Constantin, J., Grelle, A., Ibrom, A., ja Morgenstern, K. 1999. Flux partitioning between understorey and overstorey in a boreal spruce/pine forest determined by the eddy covariance method. *Agric. For. Meteorol.* **98–99**, 629–643.

De Bruin, H. A. R., Kohsiek, W. and Van Den Hurk, J. J. M. 1993. A verification of some methods to determine the fluxes of momentum, sensible heat, and water vapor using standard deviation and structure parameter of scalar meteorological quantities. *Boundary-Layer Meteorol*. **63**, 231–257.

Eugster, W., Kling, G., Jonas, T., McFadden, J. P., Wüest, A. and co-authors. 2003. CO_2 exchange between air and water in an Arctic Alaskan and midlatitude Swiss lake: importance of convective mixing. *J. Geophys. Res.* **108**(D12), 4362, doi: 10.1029/2002JD002653.

Finnigan, J. 2004. The footprint concenpt in complex terrain. *Agric. For. Meteorol.* **127**, 117–129.

Foken, T. 2006. 50 years of te Monin-Obukhov similarity theory. *Boundary-Layer Meteorol.* **119**, 431–447.

Foken, T. H., and Wichura, B. 1996. Tools for quality assessment of surface-based flux measurements. *Agric. For. Meteorol.* **78**, 83–105.

Grimmond, C. S. B., King, T. S., Cropley, F. D., Nowak, D. J. and Souch, C. 2002. Local-scale fluxes of carbon dioxide in urban environments:

methodological challenges and results from Chicago. *Environ. Pollut.* **116**, 243–254.

Grimmond, C. S. B. and Oke, T. 1999. Aerodynamic Properties of Urban Areas Derived from Analysis of Surface Form. *J. Appl. Meteorol.* **38**, 1262–1292.

Grimmond, C. S. B., Salmond, J. A., Oke, T. R., Offerle, B. and Lemonsu, A. 2004. Flux and turbulence measurements at a dense urban site in Marseille: heat, mass (water, carbon dioxide) and momentum. *J. Geophys. Res.* **109**(D24), D24101, doi: 10.1029/2004JD004936.

Kaimal, J. C. and Kristensen, L. 1991. Time series tapering for short data samples. *Boundary-Layer Meteorol.* **57**, 187–194.

Kolari, P., Kulmala, L., Tupek, B., Alm, J., Hari, P. and co-authors. 2005. Photosynthetic production of boreal forest floor vegetation; seasonal and spatial variation. *Proceedings of BACCI, NECC and FCoE activities 2005*, Book A, Finnish Association for Aerosol Research, 249–254.

Lilleberg, I. and Hellman, T. 2006. *Traffic trends in Helsinki in 2005 (in Finnish)*. Helsinki City Planning Department.

Markkanen, T., Rannik, Ü., Keronen, P., Suni, T. and Vesala, T. 2001. Eddy covariance fluxes over a boreal Scots pine forest. *Boreal Env. Res.* **6**, 65–78.

Moriwaki, R. and Kanda, M. 2004. Seasonal and diurnal fluxes of radiation, heat, water vapour, and carbon dioxide over a suburban Area. *J. Appl. Meteorol.* **43**, 1700–1710.

Markkanen, T., Rannik, Ü., Marcolla, B., Cescatti, A. and Vesala, T. 2003. Footprints and feches for fluxes over forest canopies with varying structure and density. *Boundary-Layer Meteorol.* **106**, 437–459.

Myllynen, M., Aarnio, P., Koskentalo, T. and Malkki, M. 2006. *Air Quality in Helsinki Metropolitan Area year in 2005 (in Finnish)*. YTV Helsinki Metropolitan Area Council.

Mäkelä, K., Laurikko, J. and Kanner, H. 2005. *Road traffic exhaust gas emissions in Finland. LIISA 2004 calculation software (in Finnish)*. Technical Research Centre of Finland, Buildings and Transport, Research Report RTE 2881/05.

Nemitz, E., Hargreaves, K. J., McDonald, A. G., Dorsey, J. R. and Fowler, D. 2002. Micrometeorological measurements of the urban heat budget and CO_2 emissions on a city scale. *Environ. Sci. Technol.* **36**, 3139–3146.

Rannik, Ü., Altimir, N., Raittila, J., Suni, T., Gaman, A. and co-authors. 2002. Fluxes of carbon dioxide and water vapour over Scots pine forest and clearing. *Agric. For. Meteorol.* **111**, 187–202.

Roth, M. 2000. Review of atmospheric turbulence over cities. *Quart. J. Roy. Meteorol. Soc*. **126**, 941–990.

Roth, M. and Oke, T. R. 1995. Relative efficiencies of turbulent transfer of heat, mass and momentum over a patchy urban surface. *J. Atmos. Sci.* **52**, 1863–1874.

Salmond, J. A., Oke, T. R., Grimmond, C. S. B., Roberts, S. and Offerle, B. 2005. Venting of heat and carbon dioxide from urban canyons at night. *J. Appl. Meteorol.* **44**, 1180–1194.

Schmid, H. P. 1994. Source areas for scalar and scalar fluxes. *Boundary-Layer Meteorol*. **67**, 293–318.

Schmid, H. P. 2002. Footprint modeling for vegetation atmosphere exchange studies: a review and perspective. *Agric. For. Meteorol.* **113**, 159–183.

Schuepp, P. H., Leclerc, M. Y., MacPherson, J. I. and Desjardins, R. L. 1990. Footprint prediction of scalar fluxes from analytical solutions of the diffusion equation. *Boundary-Layer Meteorol.* **50**, 355–373.

Soegaard, H. and Møller-Jensen, L. 2003. Towards a spatial CO2 budget of a metropolitan region based on textural image classification and flux measurements. *Remote Sens. Environ.* **87**, 283–294.

Sogachev, A. Y. and Lloyd, J. J. 2004. Using a one-and-a-half order closure model of the atmospheric boundary layer for surface flux footprint estimation. *Boundary-Layer Meteorol.* **112**, 467–502.

Sogachev, A. and Panferov, O. 2006. Modification of two-equation models to account for plant drag. *Boundary-Layer Meteorol.* **121**, 229–266.

Sogachev, A., Panferov, O., Gravenhorst, G. and Vesala, T. 2004b. Numerical analysis of flux footprints for different landscapes. *Theoretical and Applied Climatology* **80**, 169–185.

Sogachev, A., Rannik, Ü. and Vesala, T. 2004a. On flux footprints over the complex terrain covered by a heterogeneous forest. *Agric. For. Meteorol.* **127**, 143–158.

Sogachev, A., Menzhulin, G., Heimann, M. and Lloyd, J. 2002. A simple three-dimensional canopy – planetary boundary layer simulation model for scalar concentrations and fluxes. *Tellus* **54B**(5), 784–819.

Stull, R. B. 1988. *An introduction to boundary-layer meteorology*. Kluwer Academic Publishers.

Suni, T., Rinne, J., Reissell, A., Altimir, N., Keronen, P. and co-authors. 2003. Long-term measurements of surface fluxes above a Scot pine forest in Hyytiälä southern Finland, 1996-2001. *Boreal Environ. Res.* **8**, 287–301.

Vogt, R., Christensen, A., Rotach, M. W., Roth, M. and Satyanarayana, A. N. V. 2003. Fluxes and profiles of CO_2 in the urban roughness sublayer. Preprints, *5th International Conference on Urban Climate*, Lodz, Poland, International Association for Urban Climate, 321–324.

Vogt, R., Christensen, A., Rotach, M. W., Roth, M. and Satyanarayana, A. N. V. 2006. Temporal dynamics of CO_2 fluxes and profiles over a Central European city. *Theor. Appl. Climatol.* **84**, 117–126

Webb, E. K., Pearman, G. I. and Leuning, R. 1980. Correction of flux measurements for density effects due to heat and water vapour transfer. *Quart. J. Roy. Meteorol. Soc*. **106**, 85–100.

Wilczak, J. M., Oncley, S. P. and Stage, S. A. 2001. Sonic anemometer Tilt Correction Algorithms. *Boundary Layer Meteorol.* **99**, 127–150.